Journal of Energy and Power Engineering 11 (2017) 706-718
doi: 10.17265/1934-8975/2017.11.004

Impact of Relative Humidity of Supply Gas on Temperature Distributions in Single Cell of Polymer Electrolyte Fuel Cell When Operated at High Temperature

Akira Nishimura[1], Masato Yoshimura[1], Satoru Kamiya[1], Masafumi Hirota[1] and Eric Hu[2]

1. Division of Mechanical Engineering, Graduate School of Engineering, Mie University, Tsu-city, Mie 514-8507, Japan

2. School of Mechanical Engineering, the University of Adelaide, Adelaide, SA 5005, Australia

Received: October 20, 2017 / Accepted: October 30, 2017 / Published: November 30, 2017

Abstract: For improving the performance of stationary PEFC (polymer electrolyte fuel cell) system, the cell operating temperature up to 90 °C will be preferred in Japan during the period from 2020 to 2030. To understand the operation of the PEFC system under relatively high temperature conditions, detail heat and mass transfer analysis is required. The purpose of this study is to analyze the impact of relative humidity of supply gas on temperature distribution on the backside of separator in single cell of PEFC using Nafion membrane at higher temperature e.g. 90 °C. The in-plane temperature distribution when power was being generated was measured using thermograph with various relative humidity of supply gases. It was found that the in-plane temperature distribution at the anode was more even than that at the cathode irrespective of the relative humidity of supply gas at the anode and the cathode. The temperature elevated along gas flow through the gas channel at the cathode irrespective of relative humidity of supply gas at the anode and the cathode. The in-plane temperature distribution at the cathode was narrower with the increase in T_{ini} irrespective of relative humidity of supply gas at the cathode, while it was not observed when changing the relative humidity of supply gas at the anode. When the relative humidity of supply gas at cathode decreased, the in-plane temperature distribution at the anode was wider compared to decreasing the relative humidity of supply gas at the anode. The study concluded that the impact of relative humidity of supply gas at both anode and cathode had little impact on the in-plane temperature distribution at the cathode.

Key words: PEFC, temperature distribution, high temperature operation, relative humidity.

1. Introduction

PEFC (polymer electrolyte fuel cell) has many attractive features including high power density, quick start-up and relatively high energy conversion efficiency. However, several technical obstacles hinder its widespread commercialization for transportation and stationary application. Technical constraints on the operation of PEFC include inadequate water/humidity and heat management, intolerance to impurities such as CO, sluggish electrochemical cathode kinetics and their high cost [1].

The current PEFC has Nafion membrane and is usually operated within the temperature range between 60 °C and 80 °C [2, 3]. It is desired that PEFC operating temperature could be increased to 90 °C for stationary applications during period from 2020 to 2030 in Japan (according to NEDO road map 2010 [4]). The PEFC operated at a higher operating temperature has following merits: (1) enhancement of electrochemical kinetics for both electrode reactions; (2) simplification in the cooling system due to increase in temperature gradient between the PEFC stack and coolant; (3) increase in tolerability of CO

Corresponding author: Akira Nishimura, Ph.D., associate professor, research fields: heat transfer, fuel cell, photocatalyst and smart city.

and allowing the PEFC to use lower quality reformed hydrogen [5]. To develop the PEFC system operated under high temperature condition, heat and mass transfer characteristics should be analyzed for power generation performance and system durability.

This study focuses on the PEFC's in-plane temperature distribution as the local hot spot may cause thermal decomposition of the PEM (proton exchange membrane) and thermal stress caused by the uneven temperature distribution may break the PEM [6, 7]. It is well known that PEFC's local (generating) performance and local temperature are closely related, since operational temperature has significant impacts on electrochemical reaction kinetics, while local current density determines the local heat generation rate and thus the local temperature. Furthermore, some critical occurrences in the PEFC, such as water flooding, membrane dehydration, and even cell failure due to overheating, also depend on both local temperature and local current density [8]. Although many studies have measured the temperature distribution in a single cell of PEFC, they all used thermocouples to measure the temperature [8-12]. The insertion of thermocouples can influence the power generation performance and temperature measurement accuracy remarkably due to leakage in gases [13, 14]. Therefore, a non-contact and in-situ measurement method is promising in order to measure the temperature distribution in the cell more accurately without disturbing the heat and mass transfer phenomena during PEFC power generation. Previous studies [7, 15, 16] have reported that the results on temperature distribution (measured by non-contact thermograph) only in low operation temperature range up to 60 °C and under dry gases supply conditions. Little study has been undertaken to reveal the temperature distribution in high temperature range from 70 °C to 80 °C or even higher, except the research done by the authors [17-20].

Furthermore, the impact of relative humidity of supply gases to the anode and the cathode, on in-plane temperature distribution has never been investigated for high operation temperature range of 90 °C to 100 °C. Objective of this study is to investigate the impact. In this study, the in-plane temperature distributions on backside of separator of cell at the anode and the cathode were measured using thermograph, under power generation with various initial operational temperatures of the cell (which was equal to the temperature of supply gases at inlet) and relative humidity of supply gases. The voltage and load current were also acquired for performance analysis of PEFC.

2. PEFC Experiment System

2.1 Experimental Apparatus and Procedure

Single cell of PEFC (MC-25-SC-NH, Reactive Innovations) was used in this study in which Nafion 115 was used as PEM. The specifications of components of single cell of PEFC are given in Table 1. The in-plane temperature measurements procedure is shown in Fig. 1. The width and height of the observation window, which were equal to those of the electrode, were 50 mm and 50 mm, respectively. To prevent gas leak, the width and height of hole made in hot water passage plate were set at 40 mm and 50 mm, respectively.

The in-plane temperature distribution on the backside of separator at the anode or the cathode was measured through the observation widow using thermograph (Thermotracer TH9100WL, NIPPON AVIONICS Co., Ltd.) and analyzed by software (TH91-702, NIPPON AVIONICS Co., Ltd.). To minimize the measurement error caused by roughness and reflection of separator surface, a black body tape (HB-250, OPTIX) with thickness of 0.1 mm, was fitted on the backside of separator. The emissivity of this black body tape under this experimental condition was measured prior to the experiment. The impact on power generation output due to the observation window was very little. The pre-experiment condition

Table 1 Specifications of components of single cell of PEFC.

Parts	Size	Characteristics
PEM (Polymer electrolyte membrane)	50.0 mm × 50.0 mm × 0.13 mm	Nafion 115 (produced by Du Pont. Corp.)
Catalyst layer	50.0 mm × 50.0 mm (attached with PEM)	Pt/C (20 wt% Pt loading)
GDL (Gas diffusion layer)	50.0 mm × 50.0 mm × 0.17 mm	TGP-H060 (Carbon paper) (produced by Toray Corp.)
Separator	75.4 mm × 75.4 mm × 2.00 mm (Gas supply area: 50.0 mm × 50.0 mm)	Carbon graphite, Serpentine
Hot water passage plate	75.4 mm × 75.4 mm × 2.00 mm	Carbon graphite
Current collector	Area: 6937 mm^2, thickness: 2.00 mm	Copper coated with gold
End block	110 mm × 110 mm × 12.7 mm	Aluminum

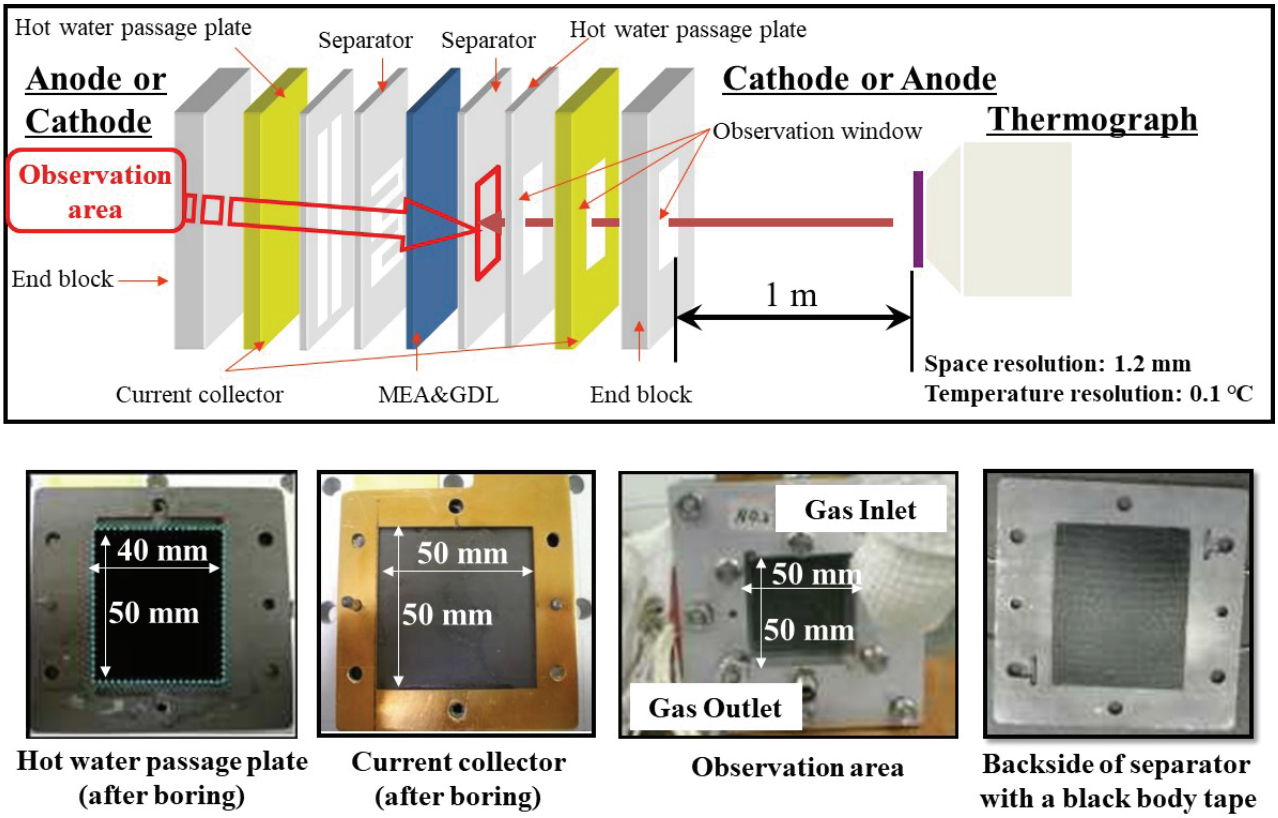

Hot water passage plate (after boring) | Current collector (after boring) | Observation area | Backside of separator with a black body tape

Fig. 1 Temperature measurement procedure of single cell of PEFC with observation window.

was taken as the initial operational temperature of cell at 70 °C and the relative humidity of both supply gases at 80% RH (with and without observation window). During the pre-experiment condition, voltages at the current density of 0.80 A/cm^2 for the anode and cathode observation were decreased by making observation window only by 4% and 7%, respectively.

In the experimental set-up, all sides of the cell, except observation window side and the opposite side to observation window, were thermally insulated. The single cell was operated at high load current density of 0.80 A/cm^2, when the in-plane temperature distribution caused by reaction heat was measured using thermograph. Under this condition, the temperature of single cell was able to be maintained over the initial operation temperature set without being heated by silicon rubber heater. In other words, the cell could maintain the temperature over the initial operation temperature with the heat generated by electrochemical reaction without external heat input.

According to the manufacturer, the thermal conductivities of PEM, GDL (gas diffusion layer) and separator are 0.195 W/(m·K), 1.7 W/(m·K) and 25 W/(m·K), respectively. Meanwhile, the thermal conductivities of hot water passage plate, current collector and end block are 25 W/(m·K), 380 W/(m·K) and 220 W/(m·K), respectively. Since the thermal conductivities of hot water passage plate, current collector and end block, which were located outside of separator, are much bigger than those of PEM, GDL and separator, it was observed that the impact of ambient air on temperature distribution was negligible. Since the gas leak had occurred without hot water passage plate, which was assembled in a commercial cell in advance, the hot water passage plate, but without flowing hot water, was introduced for preventing gas leak purposed.

The experimental conditions and parameters are given in Table 2. The experimental set-up is shown in Fig. 2. The temperatures of supply gases at the inlet of the cell were controlled to the same as initial operation temperature of cell (T_{ini}). The relative humidity of supply gases at the inlet of the cell was set in the range from 40% RH to 80% RH. The relative humidity of supply gases was managed using a humidifier and a dew point meter (HMT337FC, VAISALA). The flow rates of supply gases, which were pure H_2 for the anode and pure O_2 for the cathode, were set at the stoichiometric ratios of 1.5, 2.0 and 3.0. The flow rate of supply gases at the inlet of the cell was controlled through the mass flow controller (5850E, BROOKS INSTRUMENT). The flow rate of supply gas, which equals to the stoichiometric ratio of 1.0, is decided from Eq. (1).

Table 2 Experimental conditions.

Initial operation temperature of cell (T_{ini}) (°C)	80, 90, 100	
Load current of cell (A)	20	
(Current density of cell (A/cm^2))	(0.80)	
Supply gas condition		
	Anode	Cathode
Gas type	H_2 (purity: 99.995 vol%)	O_2 (purity: 99.995 vol%)
Temperature of supply gas at inlet (°C)	80, 90, 100	80, 90, 100
Relative humidity of supply gas (%RH)	40, 60, 80	40, 60, 80
Pressure of supply gas at inlet (absolute) (MPa)	0.4	0.4
Flow rate of supply gas at inlet (NL/min) (Stoichiometric ratio (-))	0.210 (1.5), 0.280 (2.0), 0.420 (3.0)	0.105 (1.5), 0.140 (2.0), 0.210 (3.0)

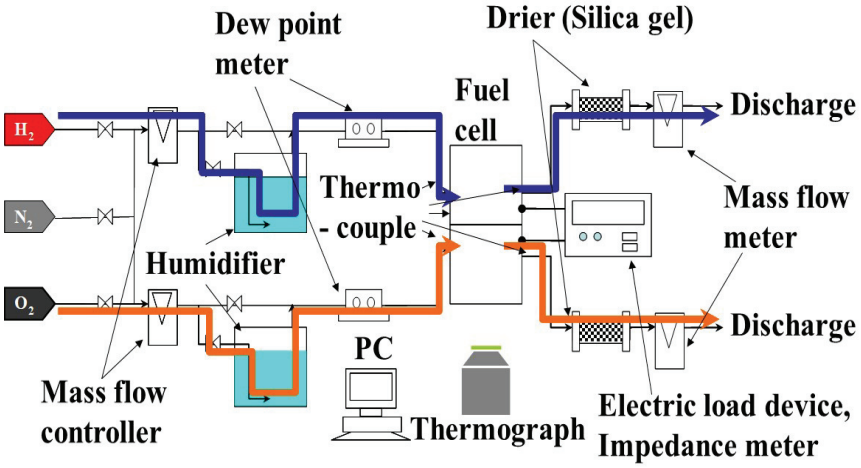

Fig. 2 Schematic drawing of experimental set-up.

$$C_{H_2} = \frac{I}{n \times F} \quad (1)$$

where C_{H_2} is the molar flow rate of supplied H_2 (mol/s), I is the load current (A) = (C/s), n is the valence ion (= 2) (-), F is Faraday constant (= 96,500) (C/mol). C_{H_2} equals to the amount of supplied H_2 of the stoichiometric ratio of 1.0. C_{O_2} which is the molar flow rate of supplied O_2 (mol/s) is half of C_{H_2}, according to Eq. (2):

$$H_2 + 1/2O_2 = H_2O \quad (2)$$

In the experimental set-up, the load current of PEFC was controlled through the electric load device (PLZ603W, KIKUSUI ELECTRONICS CORP.). Load voltage with reference to the current density was measured using the electric load device.

In this study, the single cell was heated for start-up using the silicon rubber heater (Silicon rubber heater MG, OM Heater), which was set up around the end block. In this start-up process, H_2 and O_2 were also heated at T_{ini} before being supplied into the cell. After attaining the cell temperature at T_{ini}, the power generation was started and changed through the load variation. Under the steady state loading conditions, flow rates of supply gases at the inlet and outlet of the cell and temperature distribution (measured using thermograph) were kept steady state over 30 min.

2.2 Temperature Data Analysis

In this study, the in-plane temperature distribution image obtained by using the thermograph was analyzed by segmented evaluation of cross sectional area. The in-plane temperature distribution image was divided into the area, whose vertical and horizontal length were 10 mm and 10 mm, respectively, as shown in Fig. 3. These 20 areas were named from A to T followed by the gas flow through the gas channel. The temperature averaged in each area was obtained. As to the areas of A and T, the temperature was averaged in the area, where the insulator covering the gas pipe did not disturb the detection of infrared ray by the thermograph.

Fig. 3 Schematic drawing of experimental set-up.

To evaluate the in-plane temperature distribution under the different operation conditions quantitatively, the temperature difference $T_i - T_{ave}$ (°C) has been used, where T_i is the average temperature in each area (A to T) and T_{ave} is the average temperature in whole observation area.

3. Results and Discussion

3.1 Power Generation Characteristics

Table 3 lists the average total voltage for each experimental condition. "The average total voltage" means the total voltage of the single cell obtained by averaging the data during the steady state power generation period under the specific power output operating condition. In this table, s.r. means the stoichiometric ratio. At T_{ini} of 100 °C, the power generation at the relative humidity of supply gas of 40% RH at the anode could not be carried out.

It can be seen from Table 3 that the average total voltage decreased with decrease in relative humidity of supply gases irrespective of T_{ini} except for the stoichiometric ratio and relative humidity of supply gas at the cathode are 1.5 and 40% RH, respectively at T_{ini} of 100 °C. The proton conductivity of PEM depends on water content in the Nafion membrane, which is shown in Eq. (3) [21] and it decreases with decrease in relative humidity of supply gas.

$$\sigma = (0.005139\lambda - 0.00326)\exp\left\{1268\left(\frac{1}{303} - \frac{1}{273 + T_{PEM}}\right)\right\} \quad (3)$$

where σ is the proton conductivity of PEM (Ω/cm),

Table 3 Comparison of power generation performance.

Anode	80% RH									60% RH			40% RH		
Cathode	80% RH			60% RH			40% RH			80% RH					
T_{ini} (°C)	80	90	100	80	90	100	80	90	100	80	90	100	80	90	100
s.r. = 1.5	0.45 V	0.44 V	0.25 V	0.42 V	0.38 V	0.20 V	0.35 V	0.34 V	0.23 V	0.39 V	0.31 V	0.15 V	0.34 V	0.21 V	-
s.r. = 2.0	0.44 V	0.43 V	0.25 V	0.41 V	0.37 V	0.23 V	0.35 V	0.34 V	0.21 V	0.37 V	0.29 V	0.16 V	0.32 V	0.23 V	-
s.r. = 3.0	0.43 V	0.42 V	0.26 V	0.41 V	0.36 V	0.20V	0.34 V	0.34 V	0.17 V	0.36 V	0.28 V	0.17 V	0.29 V	0.22 V	-

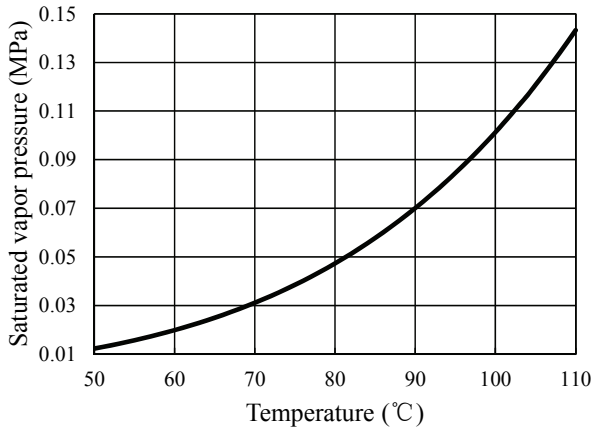

Fig. 4 Relationship between saturated vapor pressure and temperature.

λ is the water content in PEM (mol-H_2O/mol-SO_3^-), T_{PEM} is the temperature of PEM (°C). In addition, at higher T_{ini}, the saturated vapor pressure increases exponentially as shown in Fig. 4 [22]. Since the cell was heated by the power generated, the cell temperature during power generation was higher than the temperature of supply gases. If the temperature elevation is the same among the different T_{ini} conditions, the actual relative humidity in the cell decreases with increase in T_{ini} due to the exponential increase in saturation vapor pressure. Since the actual relative humidity deceased at high T_{ini}, the proton conductivity of PEM decreased, resulting in lower power generation performance.

3.2 In-plane Temperature Distribution for Changing the Relative Humidity of Supply Gas at the Cathode

Figs. 5-7 show the in-plane temperature distributions at the anode when the relative humidity of supply gas at the cathode was changed. The local temperature deviations to the average value, $T_i - T_{ave}$, are plotted for T_{ini} of 80 °C, 90 °C and 100 °C, respectively. In-plane temperature distributions at the cathode are given in Figs. 8-10 and the local temperature deviations to the average value, $T_i - T_{ave}$, are also plotted for T_{ini} of 80 °C, 90 °C and 100 °C.

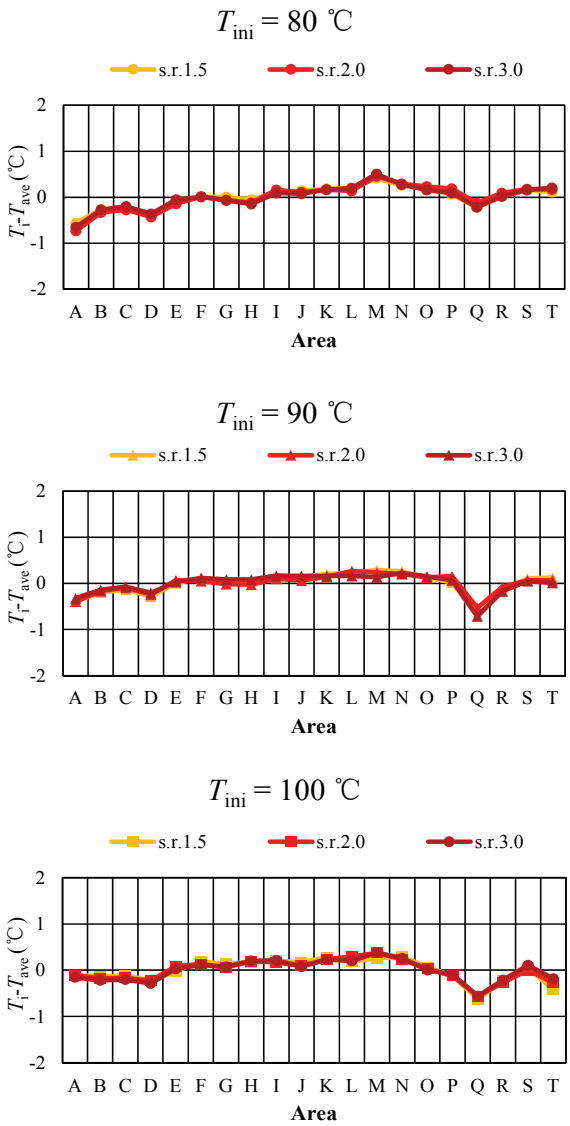

Fig. 5 In-plane temperature distribution at the anode evaluated by T_i - T_{ave} (relative humidity of supply gas at the anode: 80% RH; relative humidity of supply gas at the cathode: 80% RH).

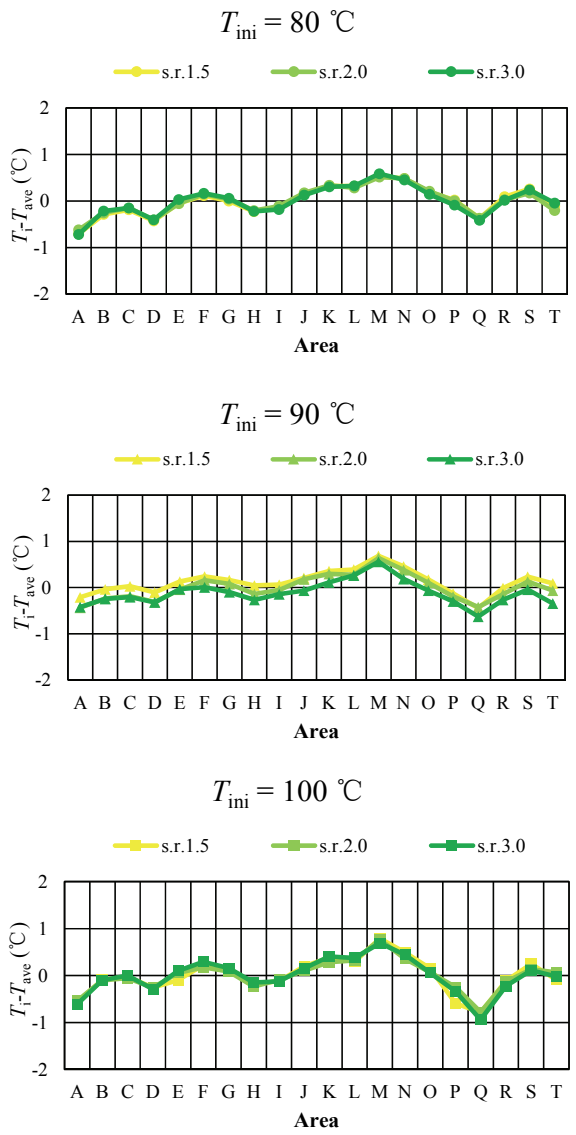

Fig. 6 In-plane temperature distribution at the anode evaluated by T_i - T_{ave} (relative humidity of supply gas at the anode: 80% RH; relative humidity of supply gas at the cathode: 60% RH).

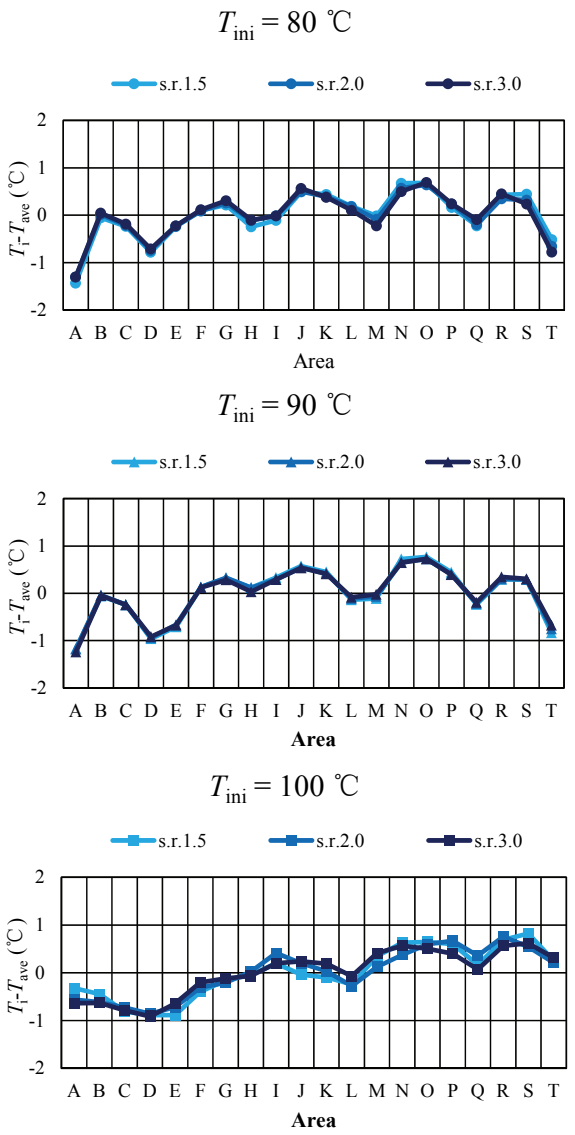

Fig. 7 In-plane temperature distribution at the anode evaluated by T_i - T_{ave} (relative humidity of supply gas at the anode: 80% RH; relative humidity of supply gas at the cathode: 40% RH).

Comparing the in-plane temperature distribution at the anode with that at the cathode, the in-plane temperature distribution at the anode was more even than that at the cathode, especially under higher relative humidity condition. The reasons are thought to be that (1) the thermal conductivity of H_2 is higher than that of O_2 [23], and (2) the flow rate of H_2 was higher than that of O_2 (Table 2) in this study. Therefore, it was considered that the convective heat transfer at the anode might be stronger than that at the cathode. On the other hand, it was observed that the temperature elevated but not significantly, along gas flow through gas channel at the cathode irrespective of T_{ini} and the relative humidity of supply gas at the cathode. Since the gas was humidified by the produced water along the gas flow, the power generation was improved by humidification of PEM, resulting in larger heat generation. On the other hand, the heat retained by sensible heat of water droplet and decrease in power generation due to gas diffusion

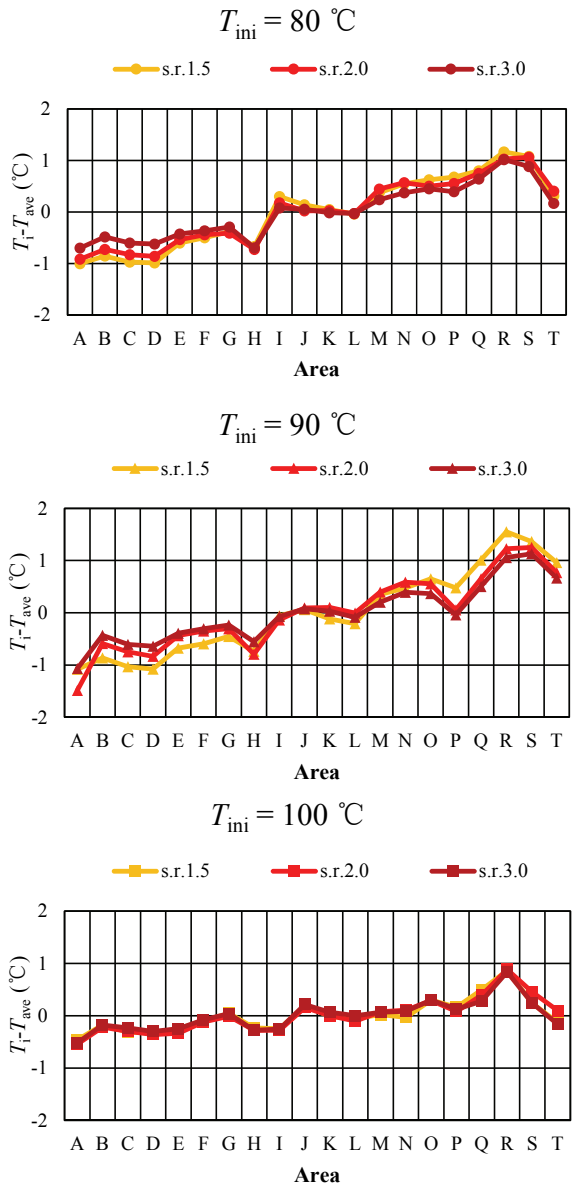

Fig. 8 In-plane temperature distribution at the cathode evaluated by T_i - T_{ave} (relative humidity of supply gas at the anode: 80% RH; relative humidity of supply gas at the cathode: 80% RH).

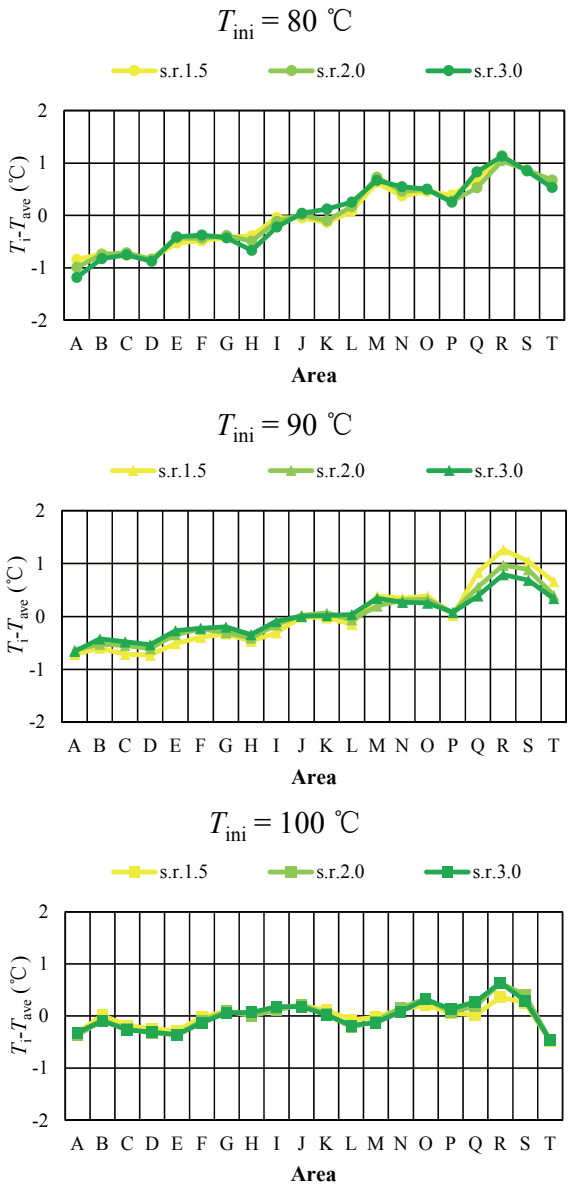

Fig. 9 In-plane temperature distribution at the cathode evaluated by T_i - T_{ave} (relative humidity of supply gas at the anode: 80% RH; relative humidity of supply gas at the cathode: 60% RH).

inhibition by liquid water might have occurred at some areas at the cathode. It was also seen that the in-plane temperature distribution at the cathode was narrower with the increase in T_{ini}. Since it was easy to be dehydrated, it was difficult to promote the power generation performance along the gas flow at higher T_{ini}.

The reason of the observed temperature drops in the areas of P or Q (in Fig. 3) for the anode and the cathode is that these areas were located at the corner of latter half of serpentine channel, the liquid waters might have been remaining there [24, 25]. In addition, it was also observed that the temperature dropped in the area of T which is the outlet of separator, and it is believed that the liquid water is easy to be accumulated there. Due to the occurrence of liquid water accumulation in GDL and gas channel in these areas, the decrease in power generation caused by gas

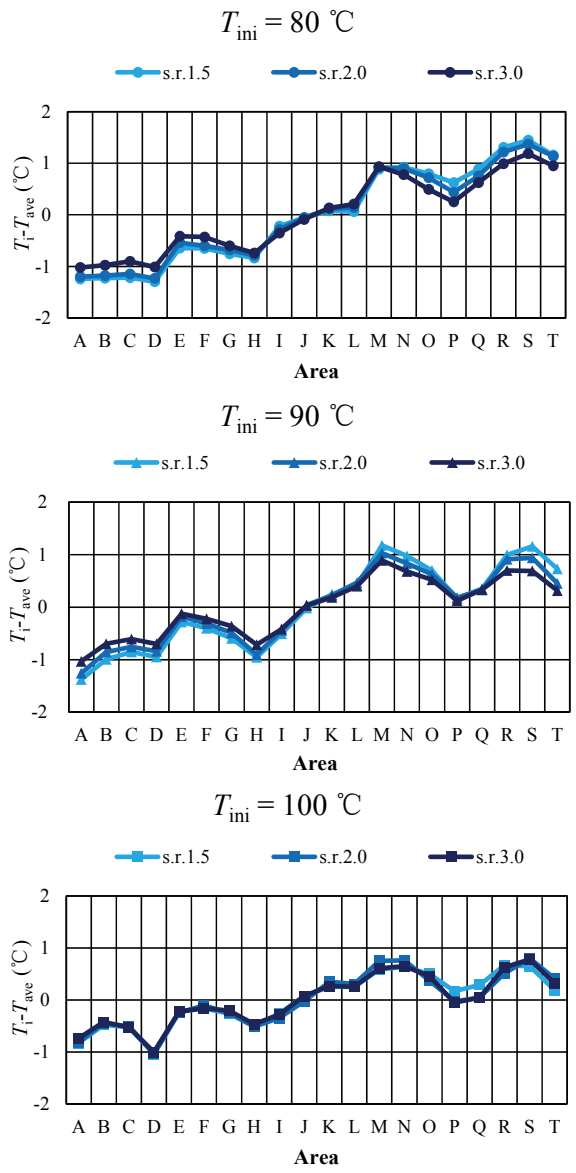

Fig. 10 In-plane temperature distribution at the cathode evaluated by T_i - T_{ave} (relative humidity of supply gas at the anode: 80% RH; relative humidity of supply gas at the cathode: 40% RH).

diffusion inhibition might have occurred. According to Ref. [26] with experimental observation of water behavior in GDL and gas channel, the cross flow in GDL might have occurred under the rib area, which promotes the power generation around the area where the liquid water is accumulated. Regarding the area of D which was opposite side through the cell, it was located at the inlet of gas flow whose temperature was colder than the cell temperature, resulting in the temperature drop.

It was observed that the in-plane temperature distribution at the anode was wider with the decrease in the relative humidity of supply gas at the cathode. The decrease makes the difference of water vapor concentration between the anode and the cathode larger, thus the water vapor transfer by diffusion from the anode to the cathode was promoted. Consequently, the power generation was promoted, resulting the temperature elevated by the generated heat. On the other hand, the impact of relative humidity of supply gas at the cathode on the in-plane temperature distribution at the cathode was little. This could be explained as that because the water vapor transfer from the anode to the cathode is caused by the osmotic drag of PEM, and the water generated by electrochemical reaction at the cathode, PEM and catalyst layer at the cathode were humidified easily even though the relative humidity of supply gas at the cathode was low. Consequently, there was little difference among the in-plane temperature distribution at the cathode under the different relative humidity of supply gases at the cathode. However, it was revealed that the larger temperature drop caused at the area of P for the condition that the relative humidity of the anode and the cathode were 80% RH and 40% RH, respectively. It was thought under this very low relative humidity condition, the humidification of PEM and catalyst layer at the cathode was not satisfactory. In addition, the gas flow rate was decreased by the gas consumption since the area of P was located in the latter half of serpentine separator. Therefore, the power generation performance was reduced, resulting in the temperature drop.

3.2 In-plane Temperature Distribution for Changing the Relative Humidity of Supply Gas at the Anode

Figs. 11-14 show the in-plane temperature distributions at the anode and the cathode with various relative humidity of the supply gases at the anode. The differences of local temperature and the whole cell

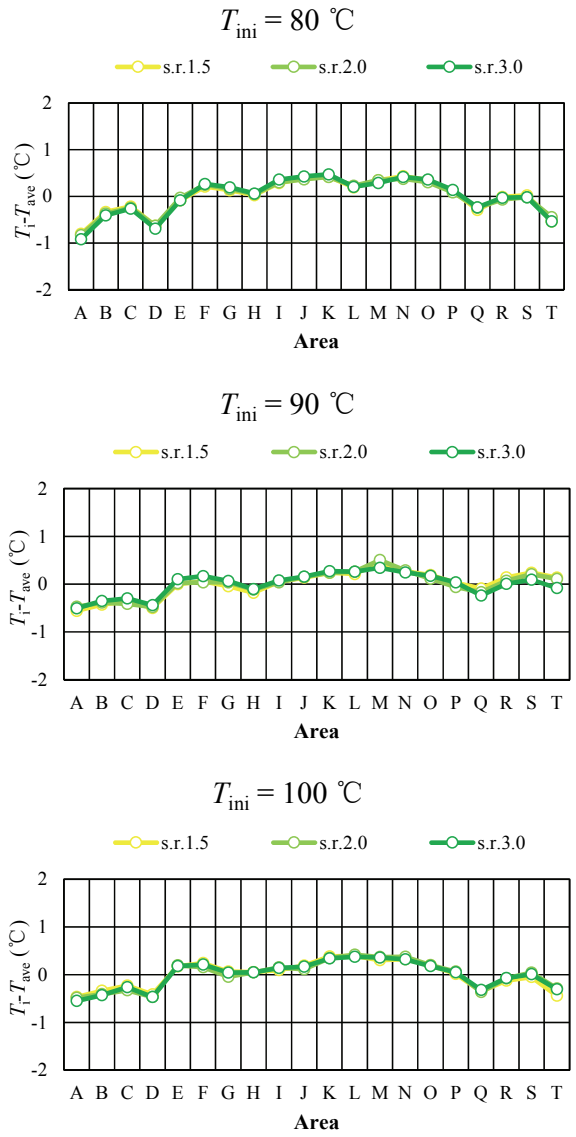

Fig. 11 In-plane temperature distribution at the anode evaluated by T_i - T_{ave} (relative humidity of supply gas at the anode: 60% RH; relative humidity of supply gas at the cathode: 80% RH).

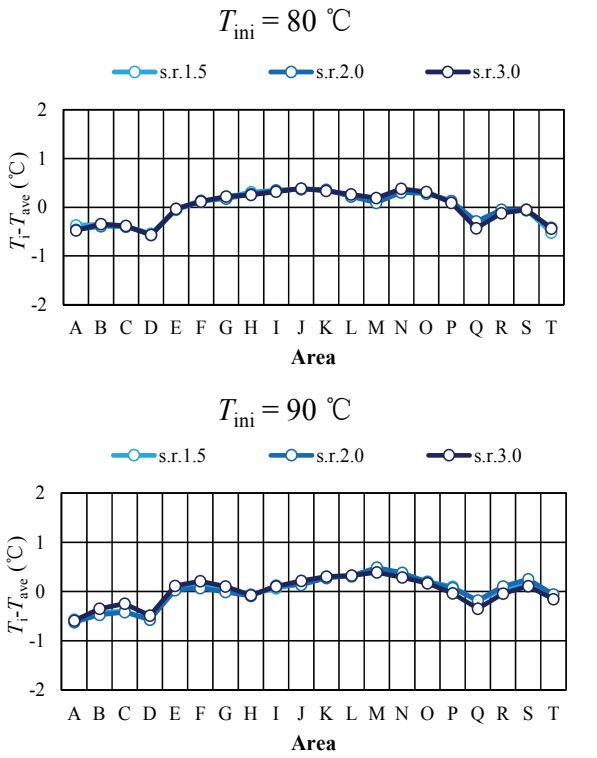

Fig. 12 In-plane temperature distribution at the anode evaluated by T_i - T_{ave} (relative humidity of supply gas at the anode: 40% RH; relative humidity of supply gas at the cathode: 80% RH).

average temperature, $T_i - T_{ave}$, are plotted for T_{ini} of 80 °C, 90 °C and 100 °C, respectively. The testing of power generation at the relative humidity of supply gas of 40% RH at the anode when T_{ini} was 100 °C could not be carried out in this study.

Comparing the in-plane temperature distribution at the anode with that at the cathode, the in-plane temperature distribution at the anode was more even than that at the cathode irrespective of T_{ini} and the relative humidity of supply gas at the anode. It was considered that the convective heat transfer at the anode might be bigger than that at the cathode as the same as the conditions changing the relative humidity of supply gas at the cathode. In addition, the temperature elevated along gas flow through the gas channel at the cathode irrespective of T_{ini} and the relative humidity of supply gas at the anode. Since the gas was humidified by the produced water along the gas channel, the power generation was improved by humidification of PEM, resulting in larger heat generation. As a result of high relative humidity of supply gas at the cathode, the O_2 reduction reaction occurred in catalyst layer at the cathode which generated the heat proceeded well even T_{ini} was 100 °C. Consequently, the temperature elevated along gas flow through gas channel at the cathode at T_{ini} of 100 °C, which was the different tendency compared to the change of the relative humidity of supply gas at the cathode.

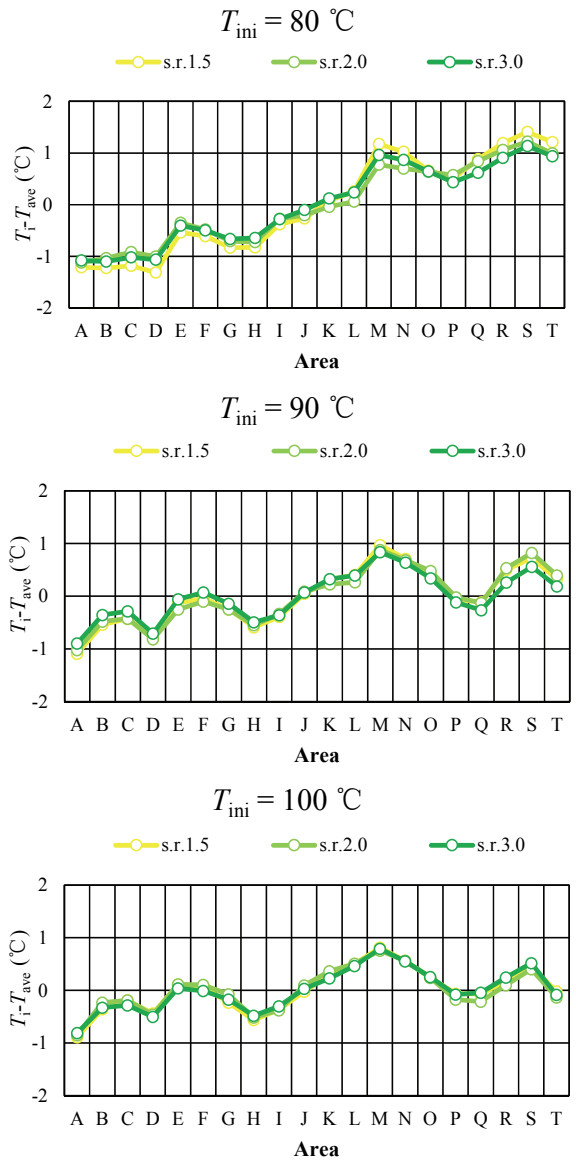

Fig. 13 In-plane temperature distribution at the cathode evaluated by T_i - T_{ave} (relative humidity of supply gas at the anode: 60% RH; relative humidity of supply gas at the cathode: 80% RH).

It was observed that the temperature dropped in the areas of P, Q and T, which was caused by the same reason described in Section 3.1. Additionally, it was also observed that the temperature dropped at the area of D due to the same reason described in Section 3.1.

It was found that the impact of relative humidity of supply gas at the anode on the in-plane temperature distribution at the anode was little. If the water vapor concentration difference from the cathode to the anode

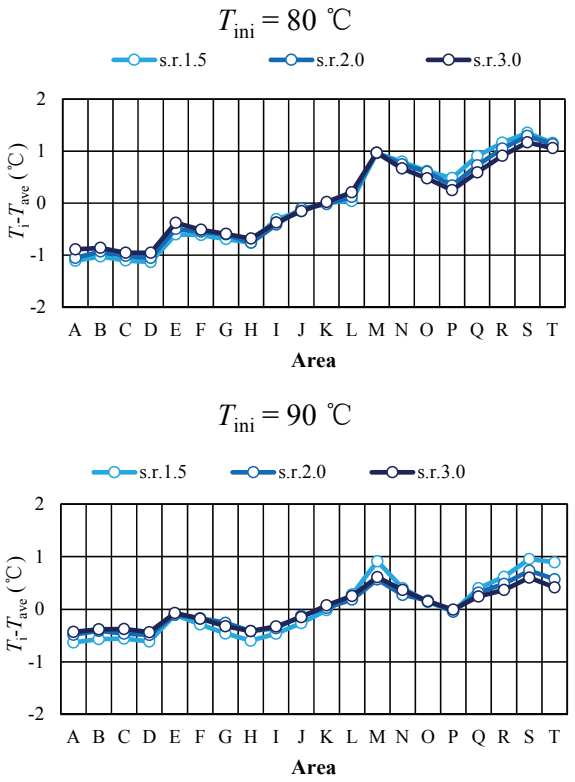

Fig. 14 In-plane temperature distribution at the cathode evaluated by T_i - T_{ave} (relative humidity of supply gas at the anode: 40% RH; relative humidity of supply gas at the cathode: 80% RH).

is high, the water vapor transfer by back diffusion might occur. Therefore, the anode side was humidified, resulting that the in-plane temperature distribution at the anode was unchanged with the different relative humidity of supply gases at the anode. In addition, it was observed that the impact of relative humidity of supply gas at the anode on the in-plane temperature distribution at the cathode was little.

The power generation performance decreased with the decrease in the relative humidity of supply gases of the anode and the cathode. It is believed that the wider temperature distribution causes the decrease in power generation performance. Therefore, it is necessary to keep the in-plane temperature distribution uniform in order to obtain the high power generation performance especially when T_{ini} is high and the relative humidity of supply gas is low. Therefore, the reuse of water discharged from the outlet of the cell by recirculation pipe line may be helpful.

4. Conclusions

In this study, the impact of relative humidity of supply gas on temperature distribution on the backside of separator in single cell of PEFC was analyzed under the power generation condition at relatively higher temperature. Based on the experimental results and analysis, the following points are concluded.

(1) It was found that the average total voltage decreased with decrease in relative humidity of supply gases irrespective of T_{ini} except for the stoichiometric ratio and relative humidity of supply gas at the cathode were 1.5% and 40% RH, respectively at T_{ini} of 100 °C.

(2) When changing relative humidity of supply gas at the anode and the cathode, the in-plane temperature distribution at the anode was more even than that at the cathode. The temperature would elevate along gas flow through the gas channel at the cathode irrespective of relative humidity of supply gas at the anode and the cathode. The in-plane temperature distribution at the cathode became narrower with the increase in T_{ini} irrespective of the relative humidity of supply gas at the cathode, while it was not observed when changing the relative humidity of supply gas at the anode.

(3) The in-plane temperature distribution at the anode became wider with the decrease in the relative humidity of supply gas at cathode, while the impact of relative humidity of supply gas at the anode on the in-plane temperature distribution at the anode was little.

(4) It could be concluded that the impact of relative humidity of supply gas at the anode and the cathode on the in-plane temperature distributions at the cathode was little.

(5) If we want to operate the PEFC using Nafion membrane under the high temperature and low relative humidity operation condition, the additional water management system is necessary.

Acknowledgments

The authors gratefully acknowledge support of the Mie Prefecture Industrial Research Institute for this study.

References

[1] Agbossou, K., Kolhe, M., Hamelin, J., Bernier, E., and Bose, T. K. 2004. "Electrolytic Hydrogen Based Renewable Energy System with Oxygen Recovery and Re-utilization." *Renewable Energy* 29 (8): 1305-18.

[2] Zhang, G., and Kandlikar, S. G. 2012. "A Critical Review of Cooling Technique in Proton Exchange Membrane Fuel Cell Stacks." *International Journal of Hydrogen Energy* 37 (February): 2412-29.

[3] Agbossou, K., Kolhe, M., Hamelin, J., and Bose, T. K. 2004. "Performance of a Stand-Alone Renewable Energy System Based on Energy Storage as Hydrogen." *IEEE Transactions on Energy Conversion* 19 (October): 633-40.

[4] NEDO (New Energy and Industry Technology Development Organization). 2010. "Road Map 2010 of NEDO Fuel Cell and Hydrogen Technology Development." Department of Fuel Cell and Hydrogen Technology. Accessed on October 11, 2017. http://www.nedo.go.jp/content/100642949.pdf.

[5] Li, Q., He, R., Jensen, J. O., and Bjerrum, N. J. 2003. "Approaches and Recent Development Polymer Electrolyte Membrane for Fuel Cells Operating above 100 °C." *Chemical of Materials* 15 (26): 4896-915.

[6] Tsuji, K. 2008. "Domestic Fuel Cell Co-generation System Entering Real Commercial Stage." *Hydrogen Energy System* 33: 93-6.

[7] Wang, M., Guo, H., and Ma, C. 2006. "Temperature Distribution on the MEA Surface of a PEMFC with Serpentine Channel Flow Bed." *Journal of Power Sources* 157 (June): 181-7.

[8] Zhang, G., Guo, L., Ma, L., and Liu, H. 2010. "Simultaneous Measurement of Current and Temperature Distributions in a Proton Exchange Membrane Fuel Cell." *Journal of Power Sources* 195 (March): 3597-604.

[9] Mizutani, C., Kitahara, T., Nakajima, H., Sasaki, K., and Ito, K. 2014. "Anallysis of Water Behavior in PEFC through 3D Thermal and Temperature Distribution Measurement by Ultrafine Thermocouples." *Transactions of the Japan Society of Mechanical Engineers* 80 (820): 1-12.

[10] Zhang, G., Shen, S., Guo, L., and Liu, H. 2012. "Dynamic Characteristics of Local Current Densities and Temperatures in Proton Exchange Membrane Fuel Cells during Reactant Starvations." *International Journal of Hydrogen Energy* 37 (2): 1884-92.

[11] Lee, C. Y., Fan, W. Y., and Chang, C. P. 2011. "A Novel Method for In-situ Monitoring of Local Voltage,

Temperature and Humidity Distributions in Fuel Cells Using Flexible Multi-functional Micro Sensors." *Sensors* 11 (2): 1418-32.

[12] Jiao, K., Alaefour, I. E., Karimi, G., and Li, X. 2011. "Simultaneous Measurement of Current and Temperature Distributions in a Proton Exchange Membrane Fuel Cell during Cold Start Processes." *Electrochimica Acta* 56 (March): 2967-82.

[13] Ogawa, T., Hohara, N., Chikahisa, T., and Hishimuar, Y. 2004. "Observation of Water Production and Temperatuer Distribution in PEM Fuel Cell." In *Proceedings of the 41st National Heat Transfer Symposium of Japan*, 235-6.

[14] Ogawa, T., Chikahisa, T., and Kikuta, K. 2003. "Measurement of Fluctuating Distribution in PEFC due to Produced Water." In *Proceedings of Thermal Engineering Conference*, 483-4.

[15] Hakenjos, A., Muenter, H., Wittstadt, U., and Hebling, C. 2004. "A PEM Fuel Cell for Combined Measurement of Current and Temperature Distribution, and Flow Field Flooding." *Journal of Power Sources* 131 (1-2): 213-6.

[16] Ogawa, T., Hohara, N., Chikahisa, T., and Hishimura, Y. 2004. "Prospect of Water Production and Temperature Distribution in PEM Fuel Cell." *Thermal Science and Engineering* 23: 93-4.

[17] Nishimura, A., Shibuya, K., Morimoto, A., Tanaka, S., Hirota, M., Nakamura, Y., Kojima, M., and Hu, E. 2012. "Dominant Factor and Mechanism of Coupling Phenomena in Single Cell of Polymer Electrolyte Fuel Cell." *Applied Energy* 90: 73-9.

[18] Nishimura, A., Shibuya, K., Morimoto, A., Tanaka, S., Hirota, M., Nakamura, Y., Kojima, M., and Narita, M. 2011. "In-situ Measurement of In-plane Temperature Distribution in a Single-Cell Polymer Electrolyte Fuel Cell Using Thermograph (1st Report: Impacts of Gas Flow Rate at Inlet and Gas Channel Pitch of Separator on In-plane Temperature Distribution and Power Generation Performance.)" *Journal of Environment and Engineering* 6 (1): 1-16.

[19] Nishimura, A., Tanaka, S., Kondo, H., and Hirota, M. 2011. "Effect Assessment of Surface Treatment and Gas Channel Pitch of Separator on In-plane Temperature Distribution and Power Generation Performance of a Single-Cell Polymer Electrolyte Fuel Cell." *Transactions of the Japan Society of Mechanical Engineers, Series B* 77 (784): 2478-91.

[20] Nishimura, A., Yoshimura, M., Mahadi, A. M., Hirota, M., and Kolhe, M. L. 2016. "Impact of Operation Condition on Temperature Distribution in Single Cell of Polymer Electrolyte Fuel Cell Operated at Higher Temperature Than Usual." *Mechanical Engineering Journal* 3 (5): 1-14.

[21] Springer, T. E., Zawodzinski, T. A., and Gottesfeld, S. 1991. "Polymer Electrolyte Fuel Cell Model." *Journal of Electrochemical Society* 138 (8): 2334-41.

[22] The Engineering Tool Box. 2017. Accessed on October 12, 2017. http://www.engineeringtoolbox.com/water-vapor-saturation-pressure-d_599.html.

[23] Japan Society of Mechanical Engineers, eds. 1993. *JSME Heat Transfer Handbook.* Tokyo: Japan Society of Mechanical Engineers, 387.

[24] Quan, P., and Lai, M. C. 2007. "Numerical Study of Water Management in the Air Flow Channel of a PEM Fuel Cell Cathode." *Journal of Power Sources* 164 (1): 223-37.

[25] Quan, P., Zhou, B., Sobiesiak, A., and Liu, Z. 2005. "Water Behavior in Serpentine Micro-channel for Proton Exchange Membrane Fuel Cell Cathode." *Journal of Power Sources* 152: 131-45.

[26] Jiao, K., Park, J., and Li, X. 2010. "Experimental Investigations on Liquid Water Removal from the Gas Diffusion Layer by Reactant Flow in PEM Fuel Cell." *Applied Energy* 87 (September): 2770-7.